Plasma Chem Plasma Process (2015) 35:831–844
DOI 10.1007/s11090-015-9633-x

ORIGINAL PAPER

Promotion of Nonthermal Plasma on the SO_2 and H_2O Tolerance of Co–In/Zeolites for the Catalytic Reduction of NO_x by C_3H_8 at Low Temperature

Hua Pan[1] · Qingfa Su[2] · Jianwen Wei[3] · Yanfei Jian[1]

Received: 14 March 2015 / Accepted: 6 June 2015 / Published online: 16 June 2015

Abstract Effects of nonthermal plasma (NTP) on the selective catalytic reduction of NO_x by C_3H_8 (C_3H_8-SCR) over Co–In/zeolites were investigated in the presence of SO_2 and H_2O at low temperatures (<below 648 K). Co–In/H-(Beta/USY) displayed the highest low-temperature activity in the NTP-facilitated C_3H_8-SCR (PF-C_3H_8-SCR) hybrid system because of the enhancement of chemisorbed oxygen, acid sites, and weak adsorption species (NO_2^- and NO_x) on Co–In/H-(Beta/USY). The assistance of NTP significantly promoted the tolerance of SO_2 and H_2O on both Co–In/H-Beta and Co–In/H-(Beta/USY) in C_3H_8-SCR reaction. Co–In/H-(Beta/USY) even exhibited excellent SO_2 tolerance in the PF-C_3H_8-SCR hybrid system when a relatively high concentration of SO_2 (1000–2000 ppm) and 7 % H_2O were introduced into the feed gas. Sulfate species formed on the active sites of Co–In/H-(Beta/USY) were unstable because of the relatively low-temperature (below 600 K) desorption of sulfate species. The unstable sulfate species contributed slight inhibition to C_3H_8 activation and nitrogen-containing formation on the active sites of Co–In/H-(Beta/USY) in the PF-C_3H_8-SCR hybrid system. The PF-C_3H_8-SCR hybrid system with Co–In/H-(Beta/USY) may be a potential candidate for DeNO$_x$ industrial applications.

Keywords Nonthermal plasma · Co–In/zeolites · NO reduction · Propane · Low temperature

✉ Qingfa Su
suqingfa@lonjing.com

✉ Jianwen Wei
jianwen988@126.com

[1] Department of Environmental Science and Engineering, Xi'an Jiaotong University, Xi'an 710049, People's Republic of China

[2] Longjing Environment Technology Co. Ltd, Xiamen 361009, People's Republic of China

[3] College of Environmental Science and Technology, Guilin University of Technology, Guilin 541004, People's Republic of China

Introduction

Selective catalytic reduction of NO_x by hydrocarbons (HC-SCR) has been one of the most promising technologies to control NO_x emissions from stationary and mobile sources since the pioneering works by Held et al. [1] and Iwamoto [2]. Among the reported catalysts, Co/Beta has attracted much attention for HC-SCR because of its high activity and N_2 selectivity [3–8]. The micropore structure of Beta zeolite, which is advantageous to intracrystalline diffusion, is considered as one of the reasons for the superiority of Co/BEA in HC-SCR [3]. The long-term thermal stability [4], loaded states of Co [5], effects of Co loading and precursor [6], preparation method [7], and reaction mechanism [8] have been widely investigated for HC-SCR on Co/Beta, especially for C_3H_8-SCR [3–7]. To improve the stability and activity of Co/zeolites in HC-SCR, many studies have focused on the modification of Co/zeolites by adding indium, such as Co–In/Beta [9], Co–In/ZSM-5 [10], Co–In/HMCM-49 [11], and Co–In/ferrierite [12]. Interestingly, Zhang et al. [13] found that Co loaded on a composite of zeolites (Beta/Y) showed higher activity than Co/Beta in CH_4-SCR because of the stronger adsorption of NO and NO_2 on Co-exchanged Beta/Y catalyst. However, Co-based zeolites, as mentioned above, only exhibited satisfactory activity in HC-SCR when the reaction temperature was more than 623 K. High reaction temperature resulted in high energy consumption. Typically, both SO_2 and H_2O are present in the flue gas from the combustion of fossil fuels. SO_2 and H_2O have been widely reported to be inhibitors of Co-based zeolites [14, 15]. Therefore, finding a solution that can improve the low-temperature activity and SO_2/H_2O tolerance of Co-based zeolites in HC-SCR is necessary.

Nonthermal plasma (NTP) can activate molecules, including NO and hydrocarbons, at ambient temperature. NO_2, formed through NO oxidation in the plasma, is more susceptible to HC-SCR at low temperatures [16]. HC is added to the stream as an $O^{\cdot}$ getter. Peroxyl radicals ($RO_2^{\cdot}$, $HO_2^{\cdot}$), which are partial oxidation products of HC conversion, allow stable conversion of NO to NO_2 without resulting in back reactions (i.e., NO_2 reduction to NO) [17, 18]. Thus, an NTP-facilitated HC-SCR (PF-HC-SCR) hybrid system is examined as a potential solution for NO_x abatement at low temperatures. Numerous investigations have been conducted on the PF-HC-SCR hybrid systems [19–23]. However, the effect of SO_2 and H_2O on the PF-HC-SCR hybrid systems has been seldom reported.

In this work, the synergistic effects of NTP on C_3H_8-SCR over Co–In/zeolites (H-Beta, H-USY, and H-Beta/USY) were investigated at temperatures ranging from 423 K to 648 K. The influences of SO_2 and H_2O on the $DeNO_x$ efficiency of the PF-C_3H_8-SCR hybrid system were studied. The reference catalysts were characterized by X-ray photoelectron spectroscopy (XPS), pyridine-infrared (Py-IR), and temperature-programmed desorption/reduction (TPD/TPR).

Materials and Methods

Catalysts Preparation

H-Beta zeolite with a SiO_2/Al_2O_3 ratio of 25 was purchased from Nankai University (China). Na-USY zeolite (Wenzhou Huahua company, Si/Al = 5.3) was ion-exchanged three times with NH_4Cl aqueous solution at 373 K for 2 h. The solid fraction was then thoroughly washed, dried at 393 K overnight, and calcined at 773 K for 4 h to obtain

H-USY zeolite. H-Beta/USY zeolite composite sample was synthesized by mixing and stirring 20 g of H-Beta and 20 g of H-USY in distilled water for 30 min at room temperature and then calcining at 413 K for 20 h.

The 3 wt% Co–3 wt% In/zeolites (H-Beta, H-USY, and H-Beta/USY) used in this study were prepared by co-impregnating the zeolites (H-Beta, H-USY, and H-Beta/USY) with a mixed aqueous solution of $Co(NO_3)_2$ and $In(NO_3)_3$ at ambient temperature for 24 h. The samples were dried at 393 K for 8 h and subsequently calcined in air at 773 K for 2 h. Finally, the catalysts were pelleted, crushed, and sieved to 40–60 mesh granulates before use. The catalyst after the SO_2 and H_2O tolerance in the PF-C_3H_8-SCR hybrid system was noted as 'catalyst aged'.

Experimental Setup

The detailed setup of the PF-C_3H_8-SCR hybrid system, which consists of a dielectric barrier discharge (DBD) plasma reactor and a fixed-bed catalytic microreactor, was described in our previous paper [9]. Approximately 3 mL of catalyst powder (weight: 1.8051 g Co–In/H-(Beta/USY), 1.8186 g Co–In/H-Beta, and 1.7902 g Co–In/H-USY) was held on a quartz frit at the center of the SCR reactor. The feeding gas composition was 700 ppm NO, 80 ppm NO_2, 8.7 % O_2, 1000 ppm C_3H_8, 13 % CO_2, 0 or 7 % H_2O, and 0–2000 ppm SO_2 and N_2 as the balance gas. Water vapor was added to the feed by bubbling N_2 through an H_2O saturator kept at 313 K. A total flow rate of 500 mL/min, which was equal to a space velocity of 10,000 h^{-1}, was maintained in the C_3H_8-SCR stage.

The NO and NO_2 concentrations were continually monitored by an NO/NO_2 analyzer. The analysis of N_2O was performed by GC with a TCD detector, which was equipped with a Porapak Q column. The N_2O byproduct formed during the NO reduction experiments was negligible (<15 ppm). Data were collected at the steady state. The catalytic activity was assessed according to the following equation:

$$\mathrm{NO_x\ conversion}\ (\%) = \frac{(\mathrm{NO_{in}} + \mathrm{NO_{2}}_{in}) - (\mathrm{NO_{out}} + \mathrm{NO_{2out}})}{\mathrm{NO_{in}} + \mathrm{NO_{2}}_{in}} \times 100\,\%, \qquad (1)$$

Catalyst Characterization

The XPS experiments were carried out on an RBD-upgraded PHI-5000C ESCA system (Perkin Elmer) with Al Kα radiation (hν = 1486.6 eV). The X-ray anode was run at 250 W with a detection angle at 54°. The pass energy was fixed at 93.90 eV to ensure sufficient resolution and sensitivity. The base pressure of the analyzer chamber was approximately 5×10^{-8} Pa. The whole spectra (0–1100 eV) and the narrow spectra of all the elements with high resolution were both recorded using RBD 147 interface through the AugerScan 3.21 software. Binding energies were calibrated by using containment carbon (C1s = 284.6 eV).

The acidity of the catalysts was determined by the pyridine adsorption–desorption method performed on a Bruker Vector 22 infrared spectrometric analyzer equipped with a DTGS detector. The spectra were recorded at a resolution of 4 cm^{-1} and with a scan number of 16. A self-supported wafer (approximately 20 mg with 16 mm diameter) was placed in an infrared cell connected to a vacuum system. Samples were evacuated at 673 K for 90 min in a vacuum (1×10^{-3} Pa). The self-supported wafer was cooled down to ambient temperature; pyridine was then adsorbed for 60 min, and the adsorbed pyridine

was evacuated at 423 K for 1 h. The catalysts were then cooled down to room temperature, and the IR spectra were obtained from 1620 to 1400 cm^{-1}.

The TPD/TPR experiment was carried out on a custom-made TCD setup using 50 mg of catalysts. Prior to the TPR experiments, samples were pretreated in pure N_2 at 723 K for 1 h. TPR was carried out with 5 K/min linear heating rate in pure N_2 with 6 % H_2 at 30 mL/min flow rate. For the NO-TPD and SO_2-TPD experiments, the catalysts were pretreated in He at 723 K for 1 h and then saturated with NO or SO_2 (4 % in He) at 30 mL/min flow rate for approximately 30 min at room temperature. Desorption was carried out by heating the sample in He (30 mL/min) at 5 K/min heating rate.

Results and Discussions

Catalytic Activity

Promotion of NTP

The effect of NTP on C_3H_8-SCR over Co–In/zeolites was examined from 423 to 648 K at 34 kV input voltage (Fig. 1). For C_3H_8-SCR without NTP assistance, Co–In/H-(Beta/USY) showed the highest catalytic activity among the Co–In/zeolite catalysts at low temperatures between 423 and 573 K. When the temperature was increased further from 573 to 623 K, the NO_x conversion of Co–In/H-Beta was higher than that of Co–In/H-(Beta/USY). Both Co–In/H-(Beta/USY) and Co–In/H-Beta could reach approximately 99 % $DeNO_x$ efficiency in C_3H_8-SCR at 648 K. However, the NO_x conversion of Co–In/H-USY catalyst was very low (<15 %) at temperatures from 423 to 573 K. When the DBD plasma reactor was turned on at 34 kV input voltage, the NO_x removal efficiency of the Co–In/

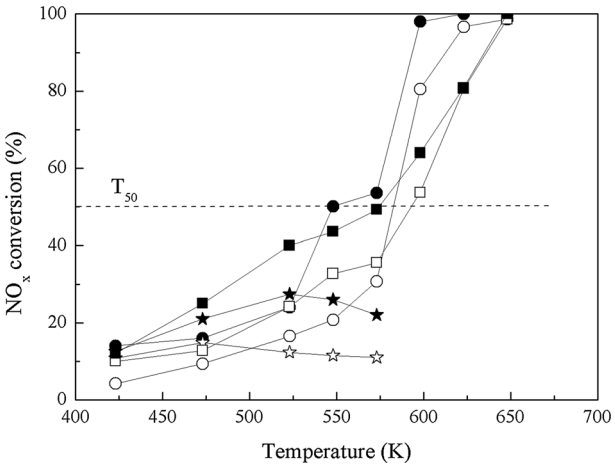

Fig. 1 The effect of NTP on C_3H_8-SCR over Co–In/H-(Beta/USY) (*filled square*, *open square*), Co–In/H-Beta (*filled circle*, *open circle*) and Co–In/H-USY (*filled star*, *open star*) from 423 to 648 K at the input voltage of 34 kV. Solid symbols (*filled square*, *filled circle* and *filled star*) indicate the results obtained in the presence of NTP and open symbols (*open square*, *open circle* and *open star*) in its absence. Reaction conditions: 700 ppm NO, 80 ppm NO_2, 1000 ppm C_3H_8, 8.7 % O_2, 13 % CO_2, balance N_2, and GHSV = 10,000 h^{-1}

zeolite catalysts was significantly enhanced at the reaction temperatures. The light-off temperature of 50 % NO_x conversion (T_{50}) for Co–In/H-(Beta/USY) and Co–In/H-Beta declined to 573 and 548 K, respectively. The synergetic effect between NTP and C_3H_8-SCR on the activity of Co–In/zeolites strongly depended on the reaction temperatures. The cofactor *R* (calculated from Eqs. 2, 3) was introduced to evaluate the synergistic effect that occurs between NTP and C_3H_8-SCR in the hybrid system at 34 kV input voltage. The effect of temperature on *R* is presented in Table 1. For Co–In/H-(Beta/USY), the hybrid system exhibited a synergistic effect between NTP and C_3H_8-SCR at low temperatures ranging from 473 to 598 K, where $R > 1$. When the temperature was higher than 623 K, $R \leq 1$, thereby indicating that the synergetic effect disappeared. For Co–In/H-Beta and Co–In/H-USY, the synergetic effect showed at temperatures from 548 to 623 K and from 523 to 573 K, respectively. According to our and other studies [9, 16, 24], the NO_2 formed through NO oxidation in the plasma is more susceptible to HC-SCR at low temperatures. In the HC-SCR reaction, the formation of NO_2 is the first important step [25–27], and subsequently the resulting NO_2 reacts with hydrocarbon-derived species to form N_2 [28] or the key intermediate species (e.g. R-NO_2, R-NCO and R-CN) [29]. Such conclusion could be also supported by the lower rate of NO/hydrocarbon reaction and the higher rate of NO_2/hydrocarbon reaction [30]. Therefore, the stable conversion of NO to NO_2 could significantly promote the NO_x conversion in HC-SCR. Under plasma discharge, C_3H_8 is added to the gas stream as an $O^{\cdot}$ getter and is decomposed into useful intermediates for NO-SCR, such as methyl (CH_3), methoxy (CH_3O) radicals, and partial oxidation products of C_3H_8 conversion including peroxyl radicals ($RO_2^{\cdot}$) and hydroperoxy radicals ($HO_2^{\cdot}$) [31, 32]. $RO_2^{\cdot}$ and $HO_2^{\cdot}$ could allow stable conversion of NO to NO_2 without the occurrence of

Table 1 Effect of temperatures on R of PF-C_3H_8-SCR hybrid system

Samples	Temperature (K)	η_{DBD} (%)[a]	η_{SCR} (%)	η_{theory} (%)	η_{hybrid} (%)	R
Co–In/H-(Beta/USY)	473	11.7	12.8	23	25	1.09
	523	11.7	24.1	33	40	1.21
	548	11.7	32.7	40.6	43.6	1.07
	573	11.7	35.6	43.1	50	1.16
	598	11.7	53.7	59.1	64	1.08
	623	11.7	80.6	82.9	80.9	0.98
	648	11.7	98.7	98.9	99	1
Co–In/H-Beta	473	11.7	9.4	20	16	0.8
	523	11.7	16.5	26.3	24	0.91
	548	11.7	20.8	30	50.1	1.67
	573	11.7	30.7	38.8	53.6	1.38
	598	11.7	80.5	82.8	98	1.18
	623	11.7	96.7	97.1	100	1.03
	648	11.7	98.7	98.9	100	1.01
Co–In/H-USY	473	11.7	14.8	24.8	21	0.85
	523	11.7	12.3	22.6	27.4	1.21
	548	11.7	11.5	21.9	26	1.19
	573	11.7	11	21.4	22	1.03

[a] η_{DBD} is the NO_x conversion of DBD reactor in the input voltage of 34 kV at room temperature [9]

back reactions [33]. In summary, NTP could promote the DeNO$_x$ efficiency of C_3H_8-SCR on Co–In/zeolites at low temperatures.

$$R = \frac{\eta_{\text{hybrid}}}{\eta_{\text{theory}}}, \tag{2}$$

$$\eta_{\text{theory}} = 1 - (1 - \eta_{\text{DBD}}) \times (1 - \eta_{\text{SCR}}), \tag{3}$$

where R is the cofactors; η_{hybrid} is the NO$_x$ conversion of the PF-C_3H_8-SCR hybrid system; η_{theory} is the theoretical value of NO$_x$ conversion, which is supposed to have no relation with the DBD plasma and C_3H_8-SCR during a series connection; η_{DBD} is the NO$_x$ conversion of the DBD reactor; and η_{SCR} is the NO$_x$ conversion of C_3H_8-SCR.

Influence of SO_2/H_2O

Figure 2 presents the effect of SO_2/H_2O on the NO$_x$ conversion of Co–In/H-Beta and Co–In/H-(Beta/USY) in the PF-C_3H_8-SCR hybrid system at 548 K. Co–In/H-USY was not studied in this section because of the low NO$_x$ conversion in the PF-C_3H_8-SCR hybrid system (Fig. 1). The NO$_x$ conversion increased significantly with NTP assistance over both catalysts in the presence of SO_2/H_2O. In C_3H_8-SCR alone, the NO$_x$ conversion decreased on both Co–In/H-Beta and Co–In/H-(Beta/USY) in the presence of 7 % H_2O. The activity of both catalysts was recovered after switching off H_2O. Interestingly, a slight promotion by 7 % H_2O was found in the PF-C_3H_8-SCR hybrid system on both Co–In/H-Beta and Co–In/H-(Beta/USY), because of NO_2 absorption by H_2O and cooling of water vapor in the DBD reactor at room temperature. With 200 ppm SO_2, an inhibition was also observed on both catalysts in C_3H_8-SCR alone. Co–In/H-(Beta/USY) showed better SO_2 tolerance than Co–In/H-Beta did in C_3H_8-SCR. When SO_2 was removed from the feed gas, the catalytic activity of both catalysts was partially recovered in C_3H_8-SCR. When the DBD reactor was turned on, the NO$_x$ conversion increased significantly on both catalysts in the presence of 200 ppm SO_2. When 7 % H_2O and 200 ppm SO_2 were added together to the gas stream, Co–In/H-Beta and Co–In/H-(Beta/USY) catalysts deactivated by SO_2 and H_2O were observed in C_3H_8-SCR alone. Compared to C_3H_8-SCR alone, a significant NTP enhancement was evidently observed over both catalysts in the presence of 7 % H_2O and 200 ppm SO_2. The suppression of the catalytic activity was mainly due to the inhibition of

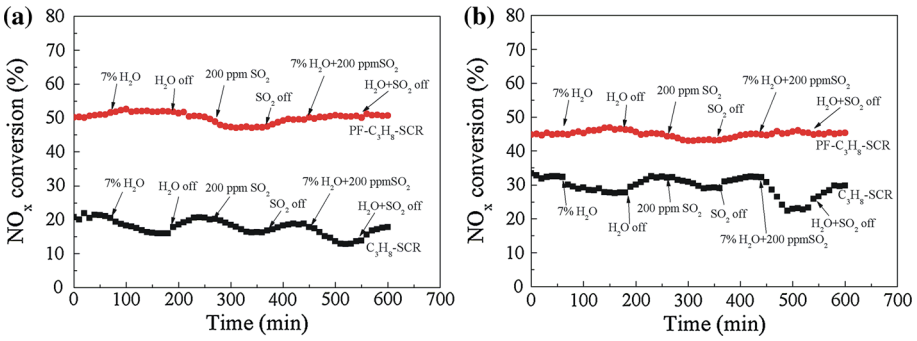

Fig. 2 The influence of SO_2/H_2O on NO$_x$ conversion over Co–In/H-Beta (**a**) and Co–In/H-(Beta/USY) (**b**) at 548 K. Reaction conditions: 700 ppm NO, 80 ppm NO_2, 1000 ppm C_3H_8, 8.7 % O_2, 13 % CO_2, 0 or 7 %H_2O, 0 or 200 ppm SO_2, balance N_2, and GHSV = 10,000 h^{-1}

HC oxidation to organic components and the suppression of nitrogen-containing formation on the active sites by SO_2 and H_2O in HC-SCR. With NTP assistance, intermediates (e.g. R-NO_2, R-NCO and R-CN) were formed during the NTP phases [34], resulting in the promotion of the SO_2 and H_2O tolerance of both catalysts in the PF-C_3H_8-SCR hybrid system.

Figure 3 illustrates the effect of SO_2 concentrations (0–2000 ppm) on the catalytic activity of Co–In/H-(Beta/USY) and Co–In/H-Beta catalysts in the PF-C_3H_8-SCR hybrid system with 7 % H_2O at 548 K during the long-term durability tests. NO_x conversion in the presence of low concentration of SO_2 (100 and 200 ppm) and 7 %H_2O is slightly higher than that in the absence of SO_2 and H_2O (Fig. 1) for both catalysts, because of NO_2 and SO_3/or SO_2 absorption by H_2O and cooling of acid (HNO_3 and H_2SO_4/or H_2SO_3) in the DBD reactor at room temperature. As shown in Fig. 3a, in the presence of high concentration of SO_2 (400–2000 ppm), the $DeNO_x$ efficiency significantly dropped to 28 % on Co–In/H-Beta. The activity loss may be attributed to the loss of active sites, which were occupied by SO_2 and surface sulfates (see section "Catalyst Characterizations"). However, the NO_x conversion gradually recovered to approximately 45 % on Co–In/H-Beta after switching off SO_2, indicating that Co–In/H-Beta catalyst is not permanently deactivated by SO_2. Compared with Co–In/H-Beta, Co–In/H-(Beta/USY) exhibited superior SO_2 tolerance (Fig. 3b). The catalytic activity of Co–In/H-(Beta/USY) was almost not influenced by high SO_2 concentration ($\leq$2000 ppm), and the NO_x conversion decreased by only 5.5 % with adding 2000 ppm SO_2 in the PF-C_3H_8-SCR hybrid system. It indicates that the PF-C_3H_8-SCR hybrid system with Co–In/H-(Beta/USY) may be a potential candidate for industrial applications.

Catalyst Characterizations

XPS

Figure 4 exhibits the XPS spectra of the elements in Co–In/zeolites. The resulting deconvolution of the Co $2p_{3/2}$ peak for the fresh and aged samples is shown in Fig. 4a. Three peaks of Co satellite (787.9 eV), Co^{2+} (782.7 eV), and oxides/silicate ad-species

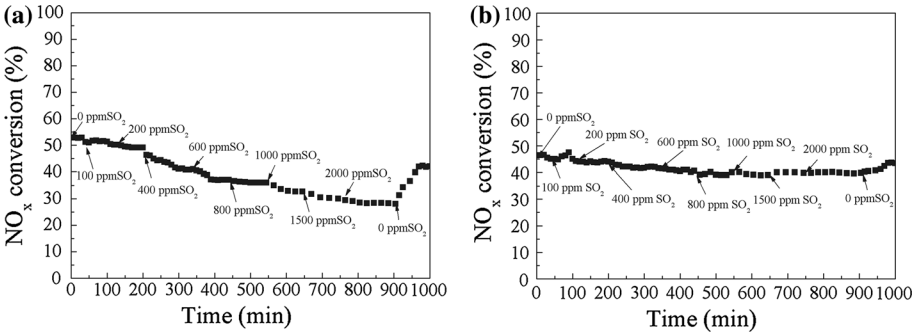

Fig. 3 The effect of SO_2 concentrations (0–2000 ppm) on the catalytic activity of Co–In/H-Beta (**a**) and Co–In/H-(Beta/USY) (**b**) catalysts in the PF-C_3H_8-SCR hybrid system with 7 % H_2O at 548 K during the long-term durability tests. Reaction conditions: 700 ppm NO, 80 ppm NO_2, 1000 ppm C_3H_8, 8.7 % O_2, 13 % CO_2, 7 %H_2O, 100–2000 ppm SO_2, balance N_2, and GHSV = 10,000 h^{-1}

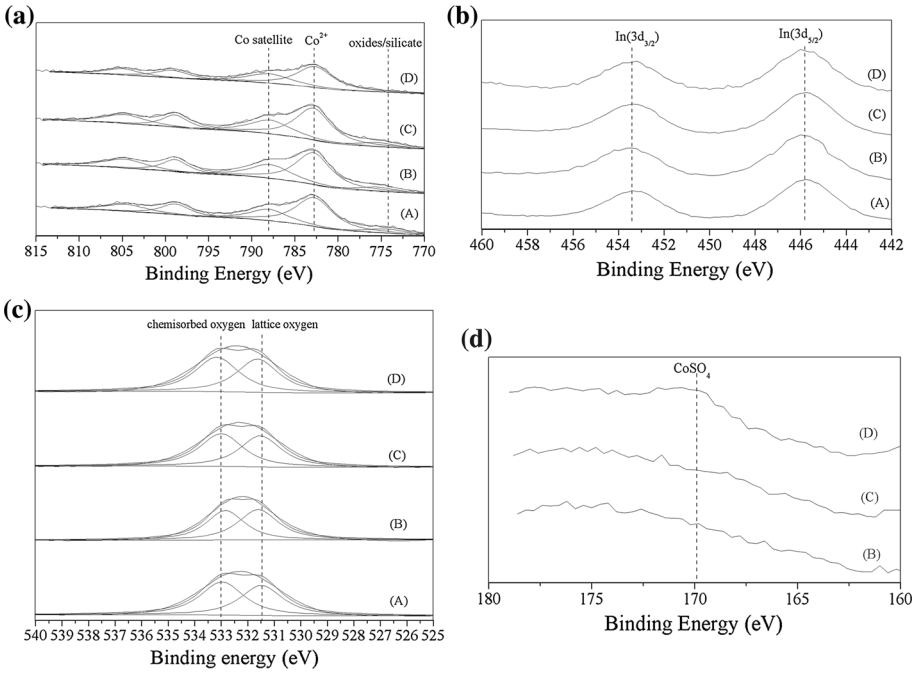

Fig. 4 XPS spectra of Co 2p (**a**), In 3d (**b**), O 1s (c) and S 1s (**d**) on Co–In/H-USY (*A*), Co–In/H-Beta (*B*), Co–In/H-(Beta/USY) (*C*), and Co–In/H-(Beta/USY) aged (*D*)

(775 eV) were detected on the fresh Co–In/H-USY, Co–In/H-Beta, and Co–In/H-(Beta/USY). The binding energies of Co_3O_4 and Co_2O_3 were not correlated exactly with those reported in the literature for pure oxides [35]. The findings indicate that a mixture of cobalt oxide species together with silicate-like species (oxides/silicate ad-species) possibly formed on the fresh Co–In/zeolites catalysts [36]. Oxides/silicate ad-species were not detected on Co–In/H-(Beta/USY) aged with SO_2 and H_2O in the PF-C_3H_8-SCR hybrid system, thereby indicating that most of them were reduced after the reaction.

The binding energy of the In $3d_{5/2}$ of Co–In/zeolites is presented in Fig. 4b. As reported by Maunula et al. [37], the binding energies of the In $3d_{5/2}$ from In_2O_3 and In^0 is 444.3 and 443.6 eV, respectively. In the Co–In/zeolite samples, the binding energies of In $3d_{5/2}$ were found at a higher binding energy of approximately 446 eV. The shift of the In $3d_{5/2}$ binding energy to a higher value was attributed to the formation of InO^+ species, according to earlier studies [37, 38]. InO^+ was proven to be the active site based on many studies [39–41]. No marked difference in the In $3d_{5/2}$ binding energy was observed between the fresh and aged Co–In/H-(Beta/USY) samples, which revealed that the indium states were not changed after reaction. This phenomenon is one of the reasons for the superior SO_2 and H_2O tolerance of Co–In/H-(Beta/USY) in the PF-C_3H_8-SCR hybrid system (Fig. 3b).

The lattice oxygen and chemisorbed oxygen were the main states of oxygen element on the catalysts. The surface chemisorbed oxygen has been reported to be the most active oxygen, which has an important role in redox reaction [42]. In Fig. 4c, deconvolution of the O 1 s peak from each sample was performed by fitting a Gaussian–Lorentzian (GL) function with a Shirley background. The O 1 s spectra for all the four samples included two peaks, with the BE value at 529.5–529.6 and 530.8–531.2 eV, respectively. The former

was ascribed to the lattice oxygen species, O^{2-} (lattice), and the latter originated from the chemisorbed oxygen species such as O_2^{2-} (ad) and/or O^- (ad) [43]. The molar ratio of the chemisorbed oxygen/lattice oxygen on the surface could be estimated from the relative areas of their XPS peaks. The ratio of chemisorbed oxygen/lattice oxygen in the surface layer of the four samples decreased in the order of Co–In/H-USY (1.14) > Co–In/H-(Beta/USY) (1.10) > Co–In/H-(Beta/USY) aged (1.08) > Co–In/H-Beta (0.91). Compared to Co–In/H-Beta, Co–In/H-(Beta/USY) showed the better catalytic activity in C_3H_8-SCR at lower temperatures below 573 K (Fig. 1), because of the promotion effect of the chemisorbed oxygen on NO oxidation and C_3H_8 activation. On the contrary, the NO_x conversion of Co–In/H-(Beta/USY) was lower than that of Co–In/H-Beta at high temperatures above 573 K (Fig. 1), because of the promotion of C_3H_8 combustion by the chemisorbed oxygen.

In Fig. 4d, the binding energy at 169.7 eV of aged Co–In/H-(Beta/USY) could be attributed to $CoSO_4$ [35]. No $CoSO_4$ was detected on the fresh Co–In/H-Beta and Co–In/H-(Beta/USY), thereby suggesting that $CoSO_4$ was generated on Co–In/H-(Beta/USY) after the SO_2 and H_2O resistance in the PF-C_3H_8-SCR hybrid system.

IR

The IR spectrum of pyridine adsorbed on Co–In/zeolites is shown in Fig. 5. The pyridine chemisorbed on Lewis and Brønsted acid sites lead to the adsorption bands at 1450 and 1540 cm^{-1} in the infrared spectra, respectively [44]. The Lewis acid site could be observed evidently on all the samples. The Brønsted acid site was detected obviously on Co–In/H-USY and Co–In/H-(Beta/USY) but not observed clearly on Co–In/H-Beta. The intensities of the Lewis and Brønsted acid sites were stronger on Co–In/H-(Beta/USY) than those on other samples. The enhancement of the acid sites might be attributed to the synergetic effect between H-Beta and H-USY zeolites with different lattice matrix structure. Similar result was also reported by Zhang et al. [13]. The Brønsted acid sites were considered as another important contributor for the improvement of the catalytic activity of Co–In/H-(Beta/USY) at low-temperature region.

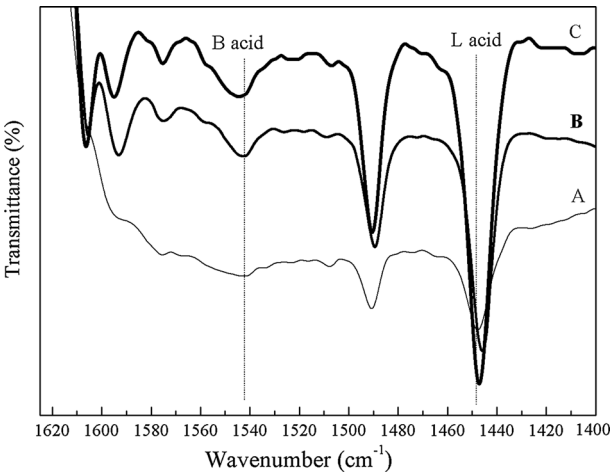

Fig. 5 Infrared spectra of pyridine adsorbed on various prepared samples: Co–In/H-Beta (*A*), Co–In/H-USY (*B*) and Co–In/H-(Beta-USY) (*C*)

H_2-TPR

The TPR results of the fresh catalysts are shown in Fig. 6. Co–In/H-Beta had three TPR peaks at 615, 735, and 1150 K, Co–In/H-USY had four TPR peaks at 593, 680, 725, and 875 K, and Co–In/H-(Beta/USY) had five peaks at 585, 650, 750, 875, and 1050 K. Reduction peaks lower than 620 K (615, 593, and 585 K) were ascribed to reducible dispersed InO^+ [45]. The peaks centered between 650 and 750 K (650, 680, 725, 735, and 750 K) could be attributed to the reduction of cobalt oxide [6]. The small peak at 875 K could be attributed to the reduction of bulk In_2O_3 phase dispersed on the internal surface of zeolites [46]. The peaks higher than 1000 K (1050 and 1150 K) were ascribed to Co^{2+} in the exchange site [15]. The InO^+ reduction peak of Co–In/H-(Beta/USY) shifted to a lower temperature (585 K) than that of Co–In/H-Beta (615 K). It indicates that InO^+ in H-(Beta/USY) zeolite matrix is unstable and easy reduction at low temperatures, resulting in the higher catalytic activity of Co–In/H-(Beta/USY) at low temperatures (Fig. 1).

TPD

Figure 7 illustrates the NO-TPD profiles on Co–In/zeolites. Co–In/H-Beta had four peaks at 420, 475, 563, and 605 K, Co–In/H-USY had two peaks at 400 and 515 K, Co–In/H-(Beta/USY) had two peaks at 437 and 570 K, and Co–In/H-(Beta/USY) aged had two peaks at 448 and 573 K. According to the literature [47], the peaks centered at the low-temperature region (375–500 K) were caused by the decomposition and desorption of weak adsorption species (NO_2^- and NO_x). The peaks centered at the high-temperature region (500–650 K) were caused by the decomposition of strong adsorption species (NO_3^-). Interestingly, NO adsorption on Co–In/H-USY and Co–In/H-(Beta/USY) mainly occurred at the low-temperature region, whereas it occurred at the high-temperature region for Co–In/H-Beta. Hence, the weak adsorption species (NO_2^- and NO_x) were adsorbed more easily on Co–In/H-(Beta/USY) and Co–In/H-USY than on Co–In/H-Beta at low temperature, suggesting that the addition of USY zeolite could promote the adsorption of NO_2^- and NO_x species on Co–In/H-(Beta/USY). By contrast, the adsorption species (NO_3^-) in Co–In/H-Beta was stronger than that in other catalysts. These different

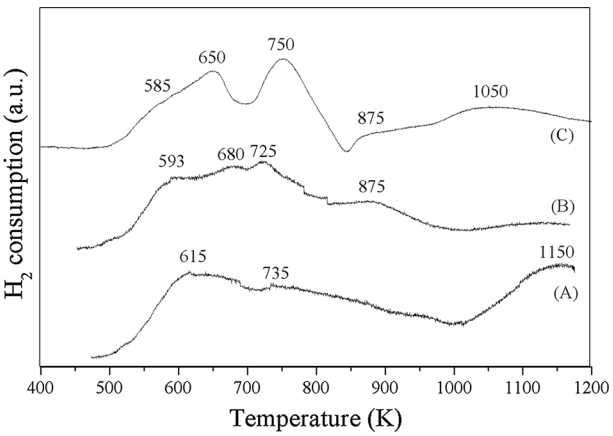

Fig. 6 H_2-TPR profiles for Co–In/H-Beta (*A*), Co–In/H-USY (*B*) and Co–In/H-(Beta/USY) (*C*)

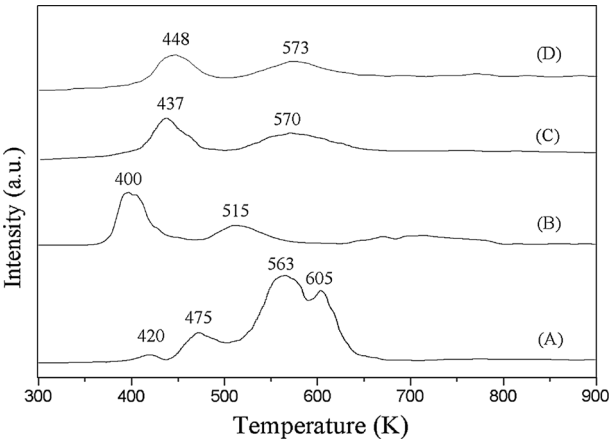

Fig. 7 NO-TPD profiles on Co–In/H-Beta (*A*), Co–In/H-USY (*B*), Co–In/H-(Beta/USY) (*C*), and Co–In/H-(Beta/USY) aged (*D*)

adsorption properties were one of the main reasons for the various catalytic activities and synergetic effect between NTP and C_3H_8-SCR on Co–In/zeolites at different temperature regions. As shown in Fig. 1, Co–In/H-(Beta/USY) showed better synergetic effect at low temperatures below 548 K, whereas Co–In/H-Beta displayed a better synergetic effect at high temperatures above 548 K. Compared to the fresh Co–In/H-(Beta/USY), the NO-TPD peaks of Co–In/H-(Beta/USY) aged slightly shifted to high temperature, and the intensity of the peaks slightly decreased. It means that NO adsorption of Co–In/H-(Beta/USY) is slightly inhibited by SO_2 and H_2O in the PF-C_3H_8-SCR hybrid system, resulting in the strong SO_2 tolerance and H_2O resistance of Co–In/H-(Beta/USY) in the PF-C_3H_8-SCR hybrid system.

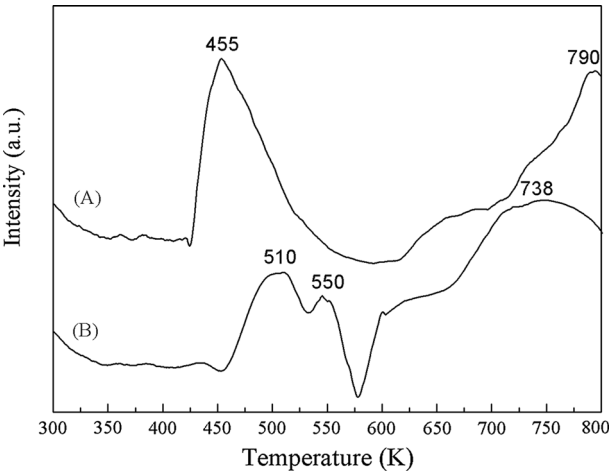

Fig. 8 SO_2-TPD profiles on fresh Co–In/H-(Beta/USY) (*A*) and Co–In/H-(Beta/USY) aged (*B*)

Figure 8 presents the results of SO_2-TPD on fresh and aged Co–In/H-(Beta/USY) with SO_2 and H_2O in the PF-C_3H_8-SCR hybrid system. The fresh Co–In/H-(Beta/USY) had two significant peaks at 455 and 790 K, and Co–In/H-(Beta/USY) aged had three obvious peaks at 510, 550, and 738 K. The peaks centered at the low-temperature region (425–600 K) were attributed to the weak adsorption of SO_2 [48]. The peaks centered at the high-temperature region above 600 K were caused by the decomposition of the sulfate species on the catalyst surface. Compared with that of fresh Co–In/H-(Beta/USY), the SO_2-TPD peaks at the low-temperature region (425–600 K) shifted to high temperature, and the intensity of the peaks decreased. This result means that the adsorption ability of SO_2 decreased after aging Co–In/H-(Beta/USY) with SO_2 and H_2O in the PF-C_3H_8-SCR hybrid system. The sulfate species formed over the active sites of Co–In/H-(Beta/USY) were unstable and contributed slightly to activity suppression because of the low-temperature (below 600 K) desorption of the sulfate species. The suppression of the catalytic activity was mainly due to the inhibition of HC oxidation to organic components, and the suppression of nitrogen-containing formation on the active sites was caused by SO_2 and H_2O. With NTP assistance, intermediates were formed during the NTP phases, resulting in the promotion of the SO_2 and H_2O tolerance of Co–In/H-(Beta/USY). Therefore, the PF-C_3H_8-SCR hybrid system with Co–In/H-(Beta/USY) may be a potential candidate for industrial applications.

Conclusions

NTP could promote the DeNO$_x$ efficiency of C_3H_8-SCR on Co–In/zeolites at low temperatures below 632 K. The synergistic effect between NTP and C_3H_8-SCR was exhibited on Co–In/H-(Beta/USY) at low temperatures ranging from 473 to 598 K, where $R > 1$. For Co–In/H-Beta and Co–In/H-USY, the synergetic effect showed at temperatures from 548 to 623 K and from 523 to 573 K, respectively. The high low-temperature activity of Co–In/H-(Beta/USY) in the PF-C_3H_8-SCR hybrid system was due to the enhancement of chemisorbed oxygen, acid sites, and weak adsorption species (NO_2^- and NO_x) on Co–In/H-(Beta/USY). The NTP assistance significantly promoted the SO_2 and H_2O tolerance on both Co–In/H-Beta and Co–In/H-(Beta/USY) in the C_3H_8-SCR reaction. When the SO_2 concentration is lower than 400 ppm, Co–In/H-Beta exhibited good SO_2 tolerance in the PF-C_3H_8-SCR hybrid system. Compared with Co–In/H-Beta, Co–In/H-(Beta/USY) exhibited superior SO_2 tolerance. The catalytic activity of Co–In/H-(Beta/USY) was almost not influenced by high SO_2 concentration ($\leq$2000 ppm). The sulfate species formed on the active sites of Co–In/H-(Beta/USY) were unstable because of the relative low-temperature (below 800 K) desorption of the sulfate species. The unstable sulfate species contributed slight inhibition to the HC oxidation to organic components and the nitrogen-containing formation on the active sites of Co–In/H-(Beta/USY). The findings suggest that the PF-C_3H_8-SCR hybrid system with Co–In/H-(Beta/USY) may be a potential candidate for DeNO$_x$ industrial applications.

Acknowledgments This work was financially supported by the National Natural Science Foundation of China (No. 21006093) and Natural Science Basic Research Plan in Shaanxi Province of China (No. 2014JQ2-2009). This project was also supported by the Guangxi Education Department Project (2013YB111) and the Fundamental Research Funds for the Central Universities.

References

1. Held W, Köning A, Richter T, Ruppe L (1990) Catalytic NO_x reduction in net oxidizing exhaust gas. SAE Paper 900496, pp 13–20
2. Iwamoto M (1990) In: Proceedings of the meeting on catalyst technology and removal of NO. Tokyo, pp 17–22
3. Tabata T, Ohtsuka H, Sabatino LMF, Bellussi G (1998) Selective catalytic reduction of NO_x by propane on Co-loaded zeolites. Microporous Mesoporous Mater 21:517–524
4. Tabata T, Kokitsu M, Ohtsuka H, Okada O, Sabatino LMF, Bellussi G (1996) Study on catalysts of selective reduction of NO_x using hydrocarbons for natural gas engines. Catal Today 27:91–98
5. Ohtsuka H, Tabata T, Okada O, Sabatino LMF, Bellussi G (1997) A study on selective reduction of NO_x by propane on Co-Beta. Catal Lett 44:265–270
6. Chen HH, Shen SC, Chen XY, Kawi S (2004) Selective catalytic reduction of NO over Co/beta-zeolite: effects of synthesis condition of beta-zeolites, Co precursor, Co loading method and reductant. Appl Catal B 50:37–47
7. Čapek L, Dědeček J, Sazama P, Wichterlová B (2010) The decisive role of the distribution of Al in the framework of beta zeolites on the structure and activity of Co ion species in propane-SCR-NO_x in the presence of water vapour. J Catal 272:44–54
8. Pietrzyk P, Dujardin C, Gora-Marek K, Granger P, Sojka Z (2012) Spectroscopic IR, EPR, and operando DRIFT insights into surface reaction pathways of selective reduction of NO by propene over the Co-BEA zeolite. Phys Chem Chem Phys 14:2203–2215
9. Shi Y, Su QF, Chen J, Wei JW, Yang JT, Pan H (2009) Combination of nonthermal plasma and low temperature-C_3H_8-selective catalytic reduction over Co–In/H-Beta catalyst for nitric oxide abatement. Environ Eng Sci 26:1107–1113
10. Lonyi F, Solt HE, Valyon J, Boix A, Gutierrez LB (2012) The SCR of NO with methane over In, H- and Co, In, H-ZSM-5 catalysts: the promotional effect of cobalt. Appl Catal B 117:212–223
11. Li F, Xiao DH, Li J, Yang X (2010) Effect of the addition of In to Co/HMCM-49 catalyst for the selective catalytic reduction of NO under lean-burn conditions. Z Phys Chem 224:907–920
12. Kubacka A, Janas J, Sulikowski B (2006) In/Co-ferrierite: a highly active catalyst for the CH_4-SCR NO process under presence of steam. Appl Catal B 69:43–48
13. Zhang J, Fan W, Liu Y, Li R (2007) Synthesis and catalytic property of a Co^{2+}-exchanged Beta/Y composite for the selective catalytic reduction of NO by CH_4 in the presence of excess oxygen. Appl Catal B 76:174–184
14. Zhang JQ, Liu YY, Fan WB, He Y, Li RF (2007) Effect of SO_2 on catalytic performance of Co-HFBZ for selective catalytic reduction of NO by CH_4 in the presence of O_2. Environ Eng Sci 24:292–300
15. Chen SW, Yan XL, Wang Y, Chen JQ, Pan DH, Ma JH, Li RF (2011) Effect of SO_2 on Co sites for NO-SCR by CH_4 over Co-Beta. Catal Today 175:12–17
16. Bamwenda GR, Obuchi A, Ogata A, Oi J, Kushiyama S, Yagita H, Mizuno K (1999) Kinetic and in situ DRIFT spectroscopy studies of NO oxidation, and reduction by C_3H_6 in excess O_2 over gamma-Al_2O_3 and Au/gamma-Al_2O_3. Stud Surf Sci Catal 121:263–268
17. Penetrante BM, Brusasco RM, Merrit BT, Pitz WJ, Vogtlin GE, Kung MC, Kung HH, Wan CZ, Voss KE (1998) Plasma-assisted catalytic reduction of NO_x. SAE Technical Paper Series #982508, SAE, Warrendale, PA
18. Dorai R, Kushner MJ (1999) Effect of propene on the remediation of NO_x from engine exhausts. SAE Technical Paper Series #1999-01-3683, SAE, Warrendale, PA
19. Niu JH, Zhang ZH, Liu DP, Wang Q (2008) Low-temperture plasma-catalytic reduction of NO_x by C_2H_2 in the presence of excess oxygen. Plasma Sour Sci Technol 10:466–470
20. Li JH, Ke R, Li W, Hao JM (2007) A comparion study on non-thermal plasma-assisted catalytic reduction of NO by C_3H_6 at low temperatures between Ag/USY and Ag/Al_2O_3 catalysts. Catal Today 126:272–278
21. Miessner H, Francke KP, Rudolph R (2002) Plasma-enhanced HC-SCR of NO_x in the presence of excess oxygen. Appl Catal B 36:53–62
22. Tran DN, Aardahl CL, Rappe KG, Park PW, Boyer CL (2004) Reduction of NO_x by plasma-facilitated catalysis over In-doped gamma-alumina. Appl Catal B 48:155–164
23. Yu QQ, Liu T, Wang H, Xiao LP, Chen M, Jiang XY, Zheng XM (2012) Cold plasma-assisted selective catalytic reduction of NO over B_2O_3/gamma-Al_2O_3. Chin J Catal 33:783–789
24. Hammer T (2002) Non-thermal plasma application to the abatement of noxious emissions in automotive exhaust gases. Plasma Sour Sci Technol 11:196–201
25. Li Y, Armor JN (1994) Selective reduction of NO_x by methane on Co-Ferrierites: I. Reaction and kinetic studies. J Catal 150:376–387

26. Lukyanov DB, Still G, d'Itri JL, Hall WK (1995) Comparison of catalyzed and homogeneous reactions of hydrocarbons for selective catalytic reduction (SCR) of NO_x. J Catal 153:265–274
27. Meunier FC, Breen JP, Zuzaniuk V, Olsson M, Ross JRH (1999) Mechanistic aspects of the selective reduction of NO by propene over alumina and silver–alumina catalysts. J Catal 187:493–505
28. Hamada H, Kintaichi Y, Inaba M, Tabata M, Yoshinari T, Tsuchida H (1996) Role of supported metals in the selective reduction of nitrogen monoxide with hydrocarbons over metal/alumina catalysts. Catal Today 29:53–57
29. Eranen K, Klingstedt F, Arve K, Lindfors LE, Murzin DY (2004) On the mechanism of the selective catalytic reduction of NO with higher hydrocarbons over a silver/alumina catalyst. J Catal 227:328–343
30. Martens JA, Cauvel A, Francis A, Hermans C, Jayat F, Remy M, Keung M, Lievens J, Jacobs PA (1998) NO_x abatement in exhaust from lean-burn combustion engines by reduction of NO_2 over silver-containing zeolite catalysts. Angew Chem Int Ed 37:1901–1903
31. Tennison P, Lambert C (2004) NO_x control development with urea SCR on a diesel passenger car. SAE Trans 113:573–579
32. Chi JN, Dacosta HFM (2005) Modeling and control of a urea-SCR after treatment system. SAE Technical Paper Series 2005-01-0966, Warrendale, PA
33. Bin G, He L, Qi C, Zhen H (2011) Removal of NO_x with selective catalytic reduction based on nonthermal plasma preoxidation. Ind Eng Chem Res 50:5401–5413
34. Nie Y, Wang JY, Zhong K, Wang LM, Guan ZC (2007) Synergy study for plasma-facilitated C_2H_4 selective catalytic reduction of NO_x over Ag/gamma-Al_2O_3 catalyst. IEEE T Plasma Sci 35:663–669
35. Wagner CD, Riggs WM, Davis LE, Moulder JF, Muilenberg GE (1979) Handbook of X-ray photoelectron spectroscopy. Perkin–Elmer Corporation, Eden Prairie
36. Chupin C, van Veen AC, Konduru M, Despres J, Mirodatos C (2006) Identity and location of active species for NO reduction by CH_4 over Co-ZSM-5. J Catal 241:103–114
37. Maunula T, Ahola J, Hamada H (2006) Reaction mechanism and kinetics of NO_x reduction by methane on In/ZSM-5 under lean conditions. Appl Catal B 64:13–24
38. Zamaro JM, Miró EE, Boix AV, Martínez-Hernández A, Fuentes GA (2010) In-zeolites prepared by oxidative solid state ion exchange (OSSIE): surface species and structural characterization. Microporous Mesoporous Mater 129:74–81
39. Beltramone AR, Pierella LB, Requejo FG, Anunziata OA (2003) Fourier transform IR study of NO + CH_4 + O_2 coadsorption on In-ZSM-5 DeNO_x catalyst. Catal Lett 91:19–24
40. Schmidt C, Sowade T, Löffler E, Birkner A, Grünert W (2002) Preparation and structure of In-ZSM-5 catalysts for the selective reduction of NO by hydrocarbons. J Phys Chem B 106:4085–4097
41. Lónyi F, Solt HE, Valyon J, Boix A, Gutierrez LB (2011) The activation of NO and CH_4 for NO-SCR reaction over In- and Co-containing H-ZSM-5 catalysts. J Mol Catal A 345:75–80
42. Kang M, Park ED, Kim JM, Yie JE (2007) Manganese oxide catalysts for NO_x reduction with NH_3 at low temperatures. Appl Catal A 327:261–269
43. Tang XF, Li YG, Huang XM, Xu YD, Zhu HQ, Wang JG, Shen WJ (2006) MnO_x–CeO_2 mixed oxide catalysts for complete oxidation of formaldehyde: Effect of preparation method and calcination temperature. Appl Catal B 62:265–273
44. Parry EP (1963) An infrared study of pyridine adsorbed on acidic solids: characterization of surface acidity. J Catal 2:371–379
45. Ramallo-López JM, Requejo FG, Gutierrez LB, Miró EE (2001) EXAFS, TDPAC and TPR characterization of PtInFerrierite: the role of surface species in the SCR of NO_x with CH_4. Appl Catal B 29:35–46
46. Ren LL (2014) The cooperative effect of In_2O_3 and In/HZSM-5 for reduction of nitric oxide with methane. J Chem 2014:1–7
47. Ferreira AP, Henriques C, Ribeiro MF, Ribeiro FR (2005) SCR of NO with methane over Co-HBEA and PdCo-HBEA catalysts—the promoting effect of steaming over bimetallic catalyst. Catal Today 107–108:181–191
48. Li JH, Zhu YQ, Ke R, Hao JM (2008) Improvement of catalytic activity and sulfur-resistance of Ag/TiO_2–Al_2O_3 for NO reduction with propene under lean burn conditions. Appl Catal B 80:202–213